Journal of the Korean Chemical Society
2013, *Vol. 57, No. 4*
Printed in the Republic of Korea
http://dx.doi.org/10.5012/jkcs.2013.57.4.461

Theoretical Study of the N-(2,5-Methylphenyl)salicylaldimine Schiff Base Ligand: Atomic Charges, Molecular Electrostatic Potential, Nonlinear Optical (NLO) Effects and Thermodynamic Properties

Tugrul C. Zeyrek*
Ankara Nuclear Research and Training Center, Turkish Atomic Energy Authority, 06100 Besevler-Ankara, Turkey
**E-mail: ctzeyrek@gmail.com*
(Received February 14, 2013; Accepted June 28, 2013)

ABSTRACT. Optimized geometrical structure, atomic charges, molecular electrostatic potential, nonlinear optical (NLO) effects and thermodynamic properties of the title compound N-(2,5-methylphenyl)salicylaldimine (I) have been investigated by using ab initio quantum chemical computational studies. Calculated results showed that the enol form of (I) is more stable than keto form. The solvent effect was investigated for obtained molecular energies, hardneses and the atomic charge distributions of (I). Natural bond orbital and frontier molecular orbital analysis of the title compound were also performed. The total molecular dipole moment (μ), linear polarizability (α), and first-order hyperpolarizability (β) were calculated by B3LYP method with 6-31G(d), 6-31+G(d,p), 6-31++G(d,p), 6-311+G(d) and 6-311++G(d,p) basis sets to investigate the NLO properties of the compound (I). The standard thermodynamic functions were obtained for the title compound with the temperature ranging from 200 to 450 K.

Key words: Density functional theory, Molecular orbitals, Schiff base, Ab initio calculations, Nonlinear optical effects

INTRODUCTION

Azomethines are known as Schiff bases which having a double C=N bond and usually synthesized from the condensation of primary amines and active carbonyl groups. Schiff bases exhibit mainly interest as corrosion inhibitors, catalyst carriers, thermo-stable materials, metal complexion agents and in biological systems and they have a wide range of applications, such as dyes and pigments.[1–9] They can be classified in terms of display interesting photochromic and thermochromic features in the solid state. This features arise via H-atom transfer from the hydroxy O atom to the imine N atom.[10,11] This H-atom transfer can be utilized for the design of several molecule based electronic devices such as measurement radiation intensity, optical computers and display systems.[12–14] Mainly, the enol-imine (OH) and the keto-amine (NH) forms of tautomeric forms are display in O-hydroxy Schiff bases (*Scheme* 1). Two types of intramolecular hydrogen bonds are observed in Schiff bases: O–H···N in enol-imine[14,15] and N–H···O in keto-amine tautomers depending on the tautomeric forms.[16,17]

Several Schiff base compounds have nonlinear optical (NLO) behaviour.[18,19] They have been under investigation the last years, since their potential applicability in optical communications. The nonlinear optical effect is based on molecular units containing highly delocalized π-electron moieties and extra electron donor and electron acceptor groups on opposite sides of the molecule at appropriate positions on the ring to enhance the conjugation. In general, Schiff base ligands consist of a variety of substituent with different electron-donating or electron withdrawing groups. Electron donor/acceptor substituent is effect on the first hyperpolarizability of Schiff base molecules.[20,21]

Density functional theory (DFT) is widely used methods in the computational quantum chemistry by using ab initio calculation of electronic structures of many particle systems. Many molecular properties calculated and revealed according to the development of better and better exchange-correlation functional method.[22] In the literature, the DFT has a great accuracy in reproducing the experimental values in geometry, dipole moment, vibrational frequency, excited states of organic compounds.[23–25]

Recently, we studied the crystal structure and conformational study by X-ray structure analysis and determined the conformational energy profiles by using AM1 semiempirical quantum mechanical method of N-(2,5-methylphenyl)salicylaldimine Schiff base ligand (I).[26] In this study, we have studied the DFT calculations for the title compound by ab initio quantum chemical calculations to investigate the molecular structural, energetic, molecular electrostatic potential, NLO and thermodynamic properties of the Schiff base compound (I).

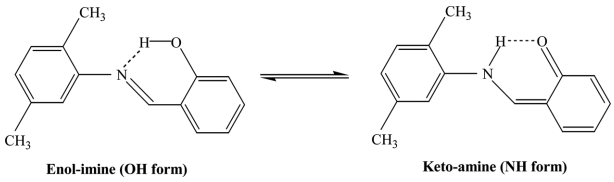

***Scheme* 1.** Tautomeric forms of the title compound.

CALCULATION DETAILS

The molecular geometry of the compound (I) is directly taken from the X-ray diffraction experimental result. This result were used at the Gaussian 03 software package and Gauss-view visualization program[27,28] for the DFT calculations with Becke's Three-parameter Hybrid Functional Using the LYP Correlation Functional B3LYP at 6-31G(d) basis set by using the Berny method.[29,30] The calculations were performed on a PC with an Intel(R) Core(TM)2 Duo CPU E4500 2.20GHz processor, 2GB RAM memory under the Microsoft Windows as the operating system.

To investigate the tautomeric stability, in gas-phase some properties such as total energy, HOMO and LUMO energies and the chemical hardness[31] of the title compound were obtained at B3LYP/6-31G(d) level. These properties were also examined in three kinds of solvent media (chloroform, ethanol and water) by using a Polarized Continuum (PCM) model.[32]

To investigate the reactive sites and to identify sites of intra- and inter-molecular interactions of the compound (I), molecular electrostatic potential surface was evaluated by using B3LYP/6-31G(d) method.

The total molecular dipole moment (μ), linear polarizability (α), and the first-order hyperpolarizability (β) by B3LYP method with different base sets [6-31G(d), 6-31+G(d,p), 6-31++G(d,p), 6-311+G(d) and 6-311++G(d,p)] for investigate the effects of basis sets on the NLO properties.

The natural bond orbital (NBO) analysis of the title compound (I) was fulfilled at the B3LYP/6-31G(d) level by means of the NBO 3.1 program within the Gaussian 03W package.[33]

Finally, the standard thermodynamic functions were obtained from statistical thermodynamics based on the vibrational frequencies analysis at B3LYP/6-31G(d) level at the Gaussian 03 software package program.

RESULTS AND DISCUSSION

Optimized Geometry

The molecular geometry of N-(2,5-methylphenyl)salicylaldimine (I) have been experimentally determined.[26] The crystallographic data of (I) has been seen orthorhombic, space group $P2_12_12_1$, with the cell dimensions a = 6.839(1), b = 7.720(4), c = 23.183(3) Å and V = 1224.1(2) Å^3. ORTEP view of the molecular structure of (I) is given in *Fig.* 1(a). The optimized parameters (bond lengths, bond angles, and dihedral angles) of the title compound (I) were obtained by using the B3LYP/6-31G(d) method (see *Fig.* 1(b)). The experimental and calculated bond distances and bond angles results are listed in *Table* 1.

The aniline ring is rotated relatively to the salicylaldi-

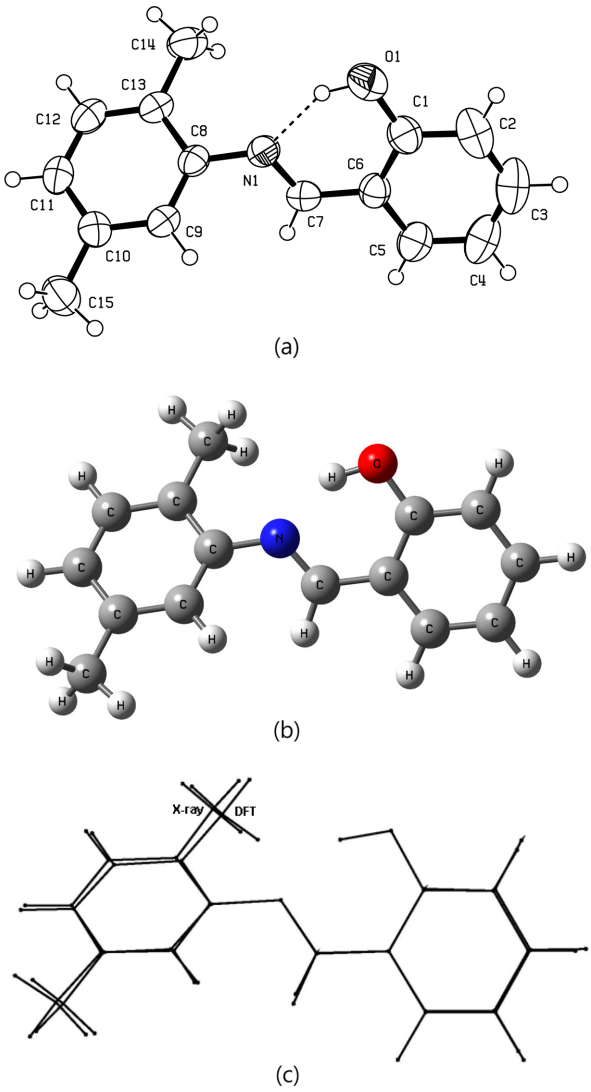

***Figure* 1.** (a) The experimental molecular structure of the title compound taken from ref 26. Displacement ellipsoids are plotted at the 50% probability level. (b) The theoretical optimized geometric structure of the title compound. (c) Superimposition of the X-ray structure of the title compound and its DFT optimized counterpart.

***Table* 1.** Optimized and experimental geometries of the title compound in the groundstate. Bond distances (Å) and angles (°) with e.s.d.s in parentheses

Parameters	Experimental [26]	Calculated 6-31G(d) B3LYP
N(1)–C(7)	1.276(2)	1.292
N(1)–C(8)	1.423(2)	1.410
O(1)–C(1)	1.346(3)	1.342
C(1)–C(2)	1.386(3)	1.403
C(1)–C(6)	1.403(3)	1.423
C(2)–C(3)	1.370(4)	1.389
C(3)–C(4)	1.372(4)	1.404
C(4)–C(5)	1.374(3)	1.386
C(5)–C(6)	1.398(3)	1.409
C(6)–C(7)	1.446(3)	1.450
C(8)–C(9)	1.393(3)	1.405
C(8)–C(13)	1.395(3)	1.411
C(9)–C(10)	1.384(3)	1.395
C(10)–C(11)	1.388(3)	1.401
C(10)–C(15)	1.503(3)	1.512
C(11)–C(12)	1.381(3)	1.394
C(12)–C(13)	1.381(3)	1.398
C(13)–C(14)	1.501(3)	1.509
Max. difference		0.032
Bond angles (°)		
C(7)–N(1)–C(8)	121.1(2)	121.1
O(1)–C(1)–C(2)	119.3(2)	118.6
O(1)–C(1)–C(6)	121.2(2)	122.0
C(2)–C(1)–C(6)	119.5(2)	119.4
C(3)–C(2)–C(1)	120.4(2)	120.2
C(2)–C(3)–C(4)	120.8(2)	121.0
C(3)–C(4)–C(5)	119.9(2)	119.1
C(4)–C(5)–C(6)	120.6(2)	121.4
C(5)–C(6)–C(1)	118.8(2)	118.9
C(5)–C(6)–C(7)	119.7(2)	119.7
C(1)–C(6)–C(7)	121.4(2)	121.4
N(1)–C(7)–C(6)	122.5(2)	122.6
C(9)–C(8)–C(13)	120.6(2)	120.1
C(9)–C(8)–N(1)	121.2(2)	121.7
C(13)–C(8)–N(1)	118.0(2)	118.1
C(10)–C(9)–C(8)	121.4(2)	121.7
C(9)–C(10)–C(11)	117.8(2)	117.9
C(9)–C(10)–C(15)	120.8(2)	121.1
C(11)–C(10)–C(15)	121.4(2)	121.0
C(12)–C(11)–C(10)	120.6(2)	120.7
C(13)–C(12)–C(11)	122.3(2)	121.9
C(12)–C(13)–C(8)	117.3(2)	117.7
C(12)–C(13)–C(14)	121.3(2)	121.2
C(8)–C(13)–C(14)	121.4(2)	121.1
Max. difference		0.8
Torsion angles (°)		
C(8)–N(1)–C(7)–C(6)	−174.4(2)	−176.9
C(9)–C(8)–N(1)–C(7)	42.6(3)	38.96
N(1)–C(7)–C(6)–C(5)	177.8(2)	179.7
C(13)–C(8)–N(1)–C(7)	−142.0(3)	−143.4
C(7)–C(6)–C(1)–O(1)	−3.0(3)	−0.2
C(3)–C(2)–C(1)–O(1)	179.9(2)	−179.8
N(1)–C(8)–C(13)–C(14)	3.0(3)	1.5
C(8)–C(9)–C(10)–C(15)	−178.7(2)	−179.5

mino-part. The aniline ring and the salicylaldimino-part are planar with a maximum deviation 0.028(2) Å. The angle of between two part is 43.3(1)°. In the structure of the title compound (I), the most important torsion angles between the aniline ring with the salicylaldimino-part are [θ_1(C8–N1–C7–C6)], [θ_2(C9–C8–N1–C7)] and [θ_3(N1–C7–C6–C5)]. From their X-ray structure determination, [θ_1(C8–N1–C7–C6)], [θ_2(C9–C8–N1–C7)] and [θ_3(N1–C7–C6–C5)] values were obtained −174.4(2)°, 42.6(3)° and 177.8(2)°, respectively. This angles have been calculated at −176.9°, 39.0° and −179.7° for the B3LYP/6-31G(d) level in the optimized structure. The conformational discrepancies between the X-ray structure and optimized counterparts can be seen from *Fig.* 1(c). The orientation of methoxy group for C14 is remarkable discrepancy between this counterparts and the orientation of this methoxy group is defined by torsion angle N1–C8–C13–C14 with value 3.0(3)° for X-ray, respectively. This torsion angle has been calculated at 1.52° for the B3LYP/6-31G(d) base sets. In the title compound (I), a strong intramolecular hydrogen bonding occurs between the hydroxyl oxygen atom and the azomethine nitrogen atom. The O1···N1 distance of 2.604(2) Å is indicative of strong intramolecular hydrogen bonding. The O1–H1 and H1···N1 distances are 0.95(3) and 1.73(3) Å, and the O1–H1···N1 angle is 150.0(2)° respectively.[26] The existence of the H-bond appears as an important property of the molecule for stabilizing its conformation in the crystal; as shown in the molecular modelling part, this is also visible in the model, obtained for the molecule discussed. The geometry of hydrogen bond in the optimized structures is examined for B3LYP. The proton donor group O1–H1 forms an intramolecular interaction with nitrogen atom N1, with a bond length of 1.75 Å and a bond angle of 147.6°. The bond length N1–C7 for X-ray structure and optimized structure at B3LYP is 1.276(2) and 1.292° Å which corresponds to a double bond, indicating an enolimine character of the title compound. The biggest difference of bond lengths between the experimental and the optimized values is found at C3–C4 bond with the difference being 0.032 Å, and the biggest differences for the bond angles are found as 0.80° at O1–C1–C6, C3–C4–C5 and C4–C5–C6. The intramolecular and intermolecular hydrogen bond interactions present in the compound (I) are very important for formation of the structure, according to mentioned comparisons, which the biggest differences of bond lengths and bond angles mainly occur in the groups involved in the hydrogen bonds.

As seen from *Table* 1, most of the optimized bond lengths are slightly longer than the experimental values. It

can be that the experimental results belong to the solid phase whereas theoretical calculations belong to the gas-phase. The result in the differences of bond parameters between the calculated and experimental values depend on the existence of the crystal field along with the inter-molecular interactions connects the molecules together in the solid state.[34] The calculated geometric parameters by using the B3LYP/6-31G(d) method are in good agreement with the X-ray structure, in spite of the observed differences, in general.

MEP, frontier molecular orbitals, NLO and thermochemical properties of (I) based on the optimized geometry are discussed as follows.

Energetic and Stability

Optimization calculations at B3LYP/6-31G(d) level were performed for both of the enol and keto forms of (I) to investigate the tautomeric stability. For each form, total energies, HOMO and LUMO energies, and chemical hardness (η) are also calculated with the same level of theory and the results are given in *Table* 2. As seen from *Table* 2, in gas-phase, the total energy of the enol form is lower than the keto form, whereas chemical hardness of the enol form is greater than the keto one. This indicates that the enol form of (I) is more stable than its keto form in gas-phase. Furthermore, calculations executed in three kinds of solvent (ε = 78.39, water; ε = 24.55, ethanol; ε = 4.9, chloroform) with the B3LYP/6-31G(d) level using the Polarized Continuum Model (PCM). Again as seen from *Table* 2, it can conclude that the total molecular energies obtained by PCM method decrease with the increasing polarity of the solvent.

Relation between the HOMOs–LUMOs Gap and the Chemical Hardness

The chemical hardness is useful to rationalize the relative stability and reactivity of chemical compounds. There are large HOMO–LUMO gap in the hard compounds and more stable and less reactive than soft compounds having small HOMO–LUMO gap.[35] The definitions of universal concepts of molecular structure stability and reactivity can be provided by using DFT method.[36] For definition of hardness η, following equation developed;[37,38]

$$\eta = \frac{1}{2}(I - A) \tag{1}$$

In the *equation* (1) I is the vertical ionization energy and A stands for the vertical electron affinity. According to the Koopman theorem,[39] the ionization energy and electron affinity can be equalized through HOMO and LUMO orbital energies:

$$EA = -\varepsilon_{HOMO}$$
$$IP = -\varepsilon_{LUMO} \tag{2}$$

According to the *equation* (2), the hardness corresponds to the gap between the HOMO and LUMO orbitals. Hence, the larger the HOMO-LUMO energy gaps the harder molecule.

$$\eta = \frac{1}{2}(\varepsilon_{LUMO} - \varepsilon_{HOMO}) \tag{3}$$

For enol and keto forms of the title compound (I), the chemical hardness (η) were calculated with the B3LYP/6-31G(d) base sets. The results are given in *Table* 2. The energy separation between the HOMO and LUMO is 4.0815 eV for enol form and 3.2924 eV for keto form. This large HOMO–LUMO gap for enol form suggests that high excitation energies for many of excited states, a good stability and high chemical hardness for the title compound (I). Indeed as seen from *Table* 2 the chemical hardness of the enol form (η_{enol} = 2.0408 eV) is greater than the keto one (η_{keto} = 1.6462 eV), which once again indicates that the enol form of (I) is more stable than its keto form in gas-phase, respectively.

Atomic Charge Distributions in Gas-Phase and in Solution-Phase

The Mulliken atomic charges for the non-H atoms of the compound (I) were calculated at B3LYP/6-31G(d) level in

***Table* 2.** Calculated total energies, frontier orbital energies and hardnesses

	NH form gas-phase	OH form			
	(ε = 1)	Gas-phase (ε = 1)	Chloroform (ε = 4.9)	Ethanol (ε = 24.55)	Water (ε = 78.39)
E_{TOTAL} (Hartree)	−710.61404593	−710.61963817	−710.62348068	−710.62491519	−710.62520565
E_{HOMO} (eV)	−5.2243	−5.7141	−5.5770	−5.5508	−5.5508
E_{LUMO} (eV)	−1.9319	−1.6326	−1.4421	−1.4149	−1.4149
$\lvert E_{HOMO} - E_{LUMO} \rvert$ (eV)	3.2924	4.0815	4.1349	4.1359	4.1359
η (eV)	1.6462	2.0408	2.0675	2.0680	2.0680

***Table* 3.** Atomic charges (e) of the title compound in gas-phase and solution-phase

Atom	In gas-phase ($\varepsilon = 1$) B3LYP/6-31G(d)	In solution-phase B3LYP/6-31G(d)		
		Chloroform ($\varepsilon = 4.9$)	Ethanol ($\varepsilon = 24.55$)	Water ($\varepsilon = 78.39$)
N1	−0.589116	−0.591962	−0.593396	−0.593720
O2	−0.653905	−0.668508	−0.673275	−0.674199
C1	0.311273	0.306548	0.304406	0.303947
C2	−0.164072	0.177045	−0.181766	−0.182711
C3	−0.127448	−0.137876	−0.141682	−0.142448
C4	−0.142382	−0.153672	−0.157814	−0.158639
C5	−0.197449	−0.205820	−0.209130	−0.209791
C6	0.081753	0.076905	0.074623	0.074126
C7	0.099725	0.098290	0.097455	0.097259
C8	0.237870	0.233121	0.231262	0.230874
C9	−0.220633	−0.230990	−0.235398	−0.236339
C10	0.170375	0.165067	0.162460	0.161910
C11	−0.169262	−0.179311	−0.183186	−0.183978
C12	−0.199221	−0.211015	0.215563	−0.216487
C13	0.153421	0.150067	0.148259	0.147868
C14	−0.523248	−0.529969	−0.532243	−0.532692
C15	−0.532104	−0.537007	−0.538576	−0.538875

gas-phase. In order to investigate the solvent effect selected three kinds of solvent (ε = 78.39, water; ε = 24.55, ethanol; ε = 4.9, chloroform), the atomic charge distributions of (I) were also calculated at B3LYP/6-31G(d) level. The calculated values of atomic charges of the title compound in gas-phase and solution-phase listed as shown in *Table* 3. According to the calculated Mulliken atomic charges, the N1 and O1 atoms have bigger negative atomic charges in gas-phase. On the other hand, as shown in *Table* 3, the atomic charge values of the N1 and O1 atoms in solution-phase are bigger than those in gas-phase and while their atomic charges are becoming more negative with the increase of the polarity of the solvent.

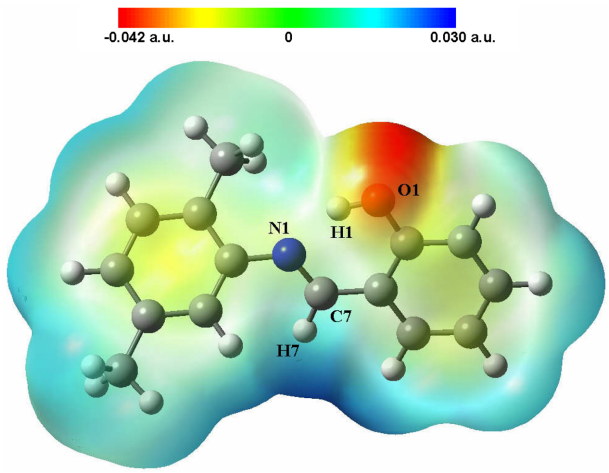

***Figure* 2.** Molecular electrostatic potential (MEP) map.

Molecular Electrostatic Potential

To investigate reactive sites for electrophilic and nucleophilic attack, the regions of the MEP for the (I) was composed by DFT calculation using the optimized geometry at the B3LYP/6-31G(d). As shown *Fig.* 2, red and yellow colours indicated for the negative regions of the MEP are related to electrophilic reactivity, while blue colours indicated for positive regions to nucleophilic reactivity. As can be seen from *Fig.* 2, compound (I) has one possible site for electrophilic attack. The oxygen atom (O1) of hydroxy group has negative region. The negative molecular electrostatic potential value is 0.042 a.u. for the mainly region of the O1 atom. The C7–H7 bond indicating a possible site for nucleophilic attack with a maximum value of 0.030 a.u. and around of this bond has maximum positive regions, respectively. According to these calculated results, the region of MEP shows that the negative potential sites are on electronegative atoms as well as the positive potential sites are around the hydrogen atoms. The determining of MEP region is best suit for identifying sites for intra- and inter-molecular interactions.[40] According to the MEP surface of the compound (I), the weak negative region associated with N1 atom and also the weak positive region by the nearby H1 atom. It can be indicative of an intramolecular (O1–H1···N1) hydrogen bonding in the compound (I).

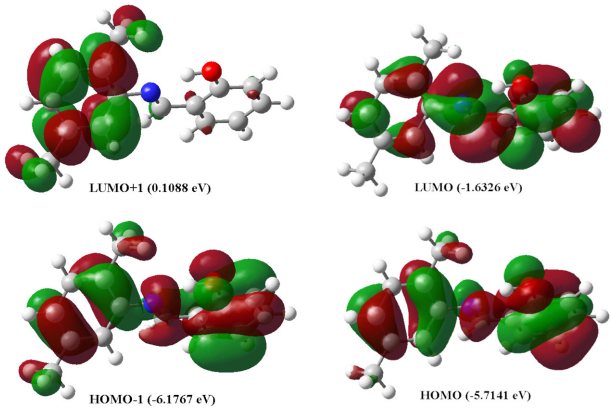

***Figure* 3.** Molecular orbital surfaces and energy levels given in parentheses for the HOMO–1, HOMO, LUMO, and LUMO+1 of the title compound computed at B3LYP/6-31G(d) level.

Frontier Molecular Orbitals

To provide a reasonable qualitative indication of the excitation properties, the highest occupied molecular orbital (HOMO) and the lowest unoccupied molecular orbital (LUMO) for the title compound were investigated. The frontier molecular orbital distributions and energy levels of the HOMO–1, HOMO, LUMO, and LUMO+1 which computed at B3LYP/6-31G(d) level of the title compound are showed in *Fig.* 3. The frontier molecular orbital shows π molecular orbital characteristics and visualized in *Fig.* 3. Except for methyl atoms of methoxy groups in the structure, the HOMO and LUMO are mainly localized on the whole structure, as seen from *Fig.* 3. The LUMO+1 is localized on 2,5-methylphenyl fragment, whereas the HOMO–1 is localized on phenol rings, the C=N atoms bond and partly methyl of methoxy groups. As seen from *Fig.* 3, both the highest occupied molecular orbitals (HOMOs) and the lowest-lying unoccupied molecular orbitals (LUMOs) are mostly the π-antibonding type molecular orbitals in the structure.

Natural Bond Orbital (NBO) Analysis

The stabilization energies of the title compound (I) were computed by using second-order perturbation theory for examined the intra and inter-molecular interactions. The stabilization energy $E^{(2)}$ connected with electron delocalization between donor $NBO_{(i)}$ and acceptor $NBO_{(j)}$ were estimated as[41]

$$E^{(2)} = -q_i \frac{(F_{ij})^2}{\varepsilon_j - \varepsilon_i} \quad (4)$$

where q_i is the donor orbital occupancy, ε_i, ε_j are diagonal elements (orbital energies) and F_{ij} is the off-diagonal NBO Fock matrix element. B3LYP/6-31G(d) level was used for Second-order perturbation theory analysis of the Fock matrix. Selected natural bond orbital occupancies of the title compound are listed in *Table* 4. The double bond N1=C7 of the structure has revealed by the NBO analysis. In aniline ring, consist of C1, C2, C3, C4, C5, C6 atoms and ring of the salicylaldimino part, consist of C9, C10, C11, C12, C13, C14 atoms are typical single-double arrangement that form the conjugate structure. Also, as seen from *Table* 4, the NBO occupancies of single C–C bonds in the ring are same level in C10–C15 and C13–C14 single bonds of methoxy groups.

***Table* 4.** Selected natural bond orbital occupancies of the title compound. BD for 2-center bond and BD* for 2-center antibond, a serial number (1, 2, ... if there is a single, double, ... bond between the pair of atoms), and the atom(s) to which the NBO is affixed

NBO	Occupancies (a.u.)	NBO	Occupancies (a.u.)
BD(1)N1 – C7	1.98738	BD*(1)N1 – C7	0.01132
BD(2)N 1 – C7	1.91674	BD*(2)N 1 – C7	0.20452
BD(1)N1 – C8	1.98234	BD*(1)N1 – C8	0.02756
BD(1)O1 – C1	1.99452	BD*(1)O1 – C1	0.01897
BD(1)C1 – C2	1.97770	BD*(1)C1 – C2	0.02382
BD(1)C1 – C6	1.97508	BD*(1)C1 – C6	0.03712
BD(2)C1 – C6	1.57294	BD*(2)C1 – C6	0.45081
BD(1)C2 – C3	1.97892	BD*(1)C2 – C3	0.01335
BD(2)C2 – C3	1.69859	BD*(2)C2 – C3	0.31271
BD(1)C3 – C4	1.98051	BD*(1)C3 – C4	0.01579
BD(1)C4 – C5	1.98060	BD*(1)C4 – C5	0.01368
BD(2)C4 – C5	1.70749	BD*(2)C4 – C5	0.31333
BD(1)C5 – C6	1.97283	BD*(1)C5 – C6	0.01965
BD(1)C6 – C7	1.97557	BD*(1)C6 – C7	0.02624
BD(1)C8 – C9	1.97342	BD*(1)C8 – C9	0.02621
BD(1)C8 – C13	1.96905	BD*(1)C8 – C13	0.03141
BD(2)C8 – C13	1.61252	BD*(2)C8 – C13	0.39403
BD(1)C9 – C10	1.97389	BD*(1)C9 – C10	0.02112
BD(2)C9 – C10	1.67191	BD*(2)C9 – C10	0.34921
BD(1)C10 – C11	1.97530	BD*(1)C10 – C11	0.02290
BD(1)C10 – C15	1.98374	BD*(1)C10 – C15	0.01553
BD(1)C11 – C12	1.97874	BD*(1)C11 – C12	0.01377
BD(2)C11 – C12	1.67358	BD*(2)C11 – C12	0.34028
BD(1)C12 – C13	1.97475	BD*(1)C12 – C13	0.02001
BD(1)C13 – C14	1.98292	BD*(1)C13 – C14	0.01503

The results of second-order perturbation theory analysis of the Fock matrix and the stabilization energies larger than 3 kcal mol^{-1} are presented in *Table* 5. Some strong intramolecular interactions, which are formed by the overlap between σ(C–C), σ*(C–C) and π(C–C), π*(C–C) bond orbital in the aromatic ring, which leads intramolecular

***Table* 5.** Second-order perturbation theory analysis of the Fock matrix in NBO basis, calculated at B3LYP/6-31G(d) level. LP for 1 center valence lone pair

Donor orbital (*i*)	Type	Acceptor orbital (*i*)	Type	$E^{(2)}$ (kcal/mol)[a]	$\varepsilon_j - \varepsilon_i$ (a.u.)[b]	F_{ij} (a.u.)[c]
C1 – C6	σ	C5 – C6	σ^*	3.31	1.25	0.058
	π	N1 – C7	π^*	22.01	0.26	0.072
	π	C2 – C3	π^*	14.52	0.28	0.059
	π	C4 – C5	π^*	22.54	0.28	0.073
C5 – C6	σ	O1 – C1	σ^*	3.48	1.09	0.055
	σ	C1 – C6	σ^*	3.32	1.22	0.057
C6 – C7	σ	N1 – C8	σ^*	4.17	1.13	0.061
C1 – C2	σ	C1 – C6	σ^*	3.07	1.23	0.055
	σ	C6 – C7	σ^*	3.01	1.19	0.054
C2 – C3	σ	O1 – C1	σ^*	3.53	1.09	0.056
C4 – C5	σ	C6 – C7	σ^*	3.06	1.20	0.054
	π	C1 – C6	π^*	14.93	0.27	0.060
	π	C2 – C3	π^*	21.86	0.29	0.071
C8 – C13	σ	C8 – C9	σ^*	3.58	1.25	0.060
C8 – C9	σ	C8 – C13	σ^*	4.17	1.26	0.065
	σ	C9 – C10	σ^*	3.27	1.28	0.058
C12 – C13	σ	C8 – C13	σ^*	3.31	1.25	0.058
C11 – C12	σ	C10 – C11	σ^*	3.01	1.27	0.055
	σ	C10 – C11	σ^*	3.40	1.11	0.055
	σ	C12 – C13	σ^*	3.06	1.27	0.056
	σ	C13 – C14	σ^*	3.30	1.11	0.054
	π	C8 – C13	π^*	19.76	0.28	0.068
	π	C9 – C10	π^*	21.08	0.28	0.070
C9 – C10	π	C8 – C13	π^*	20.59	0.28	0.070
	π	C11 – C12	π^*	18.80	0.28	0.065
C10 – C11	σ	C9 – C10	σ^*	3.32	1.27	0.058
O1	LP(1)	C1 – C6	σ^*	7.76	1.09	0.082
	LP(2)	C1 – C6	π^*	38.28	0.32	0.106
N1	LP(1)	O1 – H1	σ^*	43.90	0.50	0.145
	LP(1)	C8 – C13	π^*	4.65	0.40	0.041
	LP(1)	C7 – H7	σ^*	11.41	0.78	0.087
	LP(1)	C8 – C9	σ^*	5.48	0.92	0.066

[a]$E^{(2)}$ means energy of hyper conjugative interactions.
[b]Energy difference between donor and acceptor *i* and *j* NBO orbitals.
[c]F_{ij} is the Fock matrix element between *i* and *j* NBO orbitals.

charge transfer (ICT) causing stabilization of the system have revealed by the NBO analysis.

The strong intramolecular hyperconjugative interaction of the σ and π electrons of C–C to the anti C–C bond of the aromatic rings results to stabilization of some part of the rings as evident from *Table* 5. Such as, the intramolecular hyperconjugative interaction of the σ(C1–C6) distribute to σ^*(C5–C6) stabilization of 3.31 kcal mol^{-1}. This enhanced further conjugate with antibonding orbital π^* (N1–C7), (C2–C3) and (C4–C5) which results to strong delocalization of 22.01, 14.52 and 22.54 kcal mol^{-1}, respectively. The same kind interaction is calculated in the (C2–C3), (C4– 5), (C8–C13), (C9–C10) and (C11–C12) bonds for (I) as shown in *Table* 5. The lone pair of O1 donates its electrons to the π-type anti bonding orbital for (C1–C6). This interaction gives the strong stabilization to the system of (I) by 38.28 kcal mol^{-1}.

The NBO analysis has revealed the strongest stabilization was determined the NBO analysis in the compound (I). The strongest stabilization energy is 43.90 kcal mol^{-1} for the N1(O1)→σ(O1–H1) interaction. The electron donating from N1 LP(1) to antibonding (O1–H1) is the most important interaction energy resulting stabilization of 43.90 kcal mol^{-1}, and this interaction implies the exist-

ence of intramolecular hydrogen bond, this was observed experimentally. The same N1 LP (1) with antibonding orbital of σ*(C7–H7), σ*(C8–C9) and π*(C8–C13) leads to moderate stabilization of 11.41, 5.48 and 4.65 kcal mol^{-1}, respectively.

Nonlinear Optical (NLO) Effects

To investigate the nonlinear optical properties of the molecules is very importance because of the key functions of frequency shifting, optical modulation, optical switching, optical logic and optical memory for the emerging technologies in eras such as in telecommunications, signal processing and optical interconnections.[42]

Thanthiriwatte, and Nalin de Silva were explained in detail previously that how is the calculations of the total dipole moment (μ_{tot}), linear polarizability (α_{ij}), and the first-order hyperpolarizability (β_{ijk}) from the Gaussian output file.[43]

The total molecular dipole moment (μ), linear polarizability (α), and the first-order hyperpolarizability (β) were calculated by B3LYP method with each of 6-31G(d), 6-31+G(d,p), 6-31++G(d,p), 6-311+G(d) and 6-311++G(d,p) basis sets to investigate the effects of basis sets on the NLO properties. The calculated values of the μ_{tot}, α_{tot} and β_{tot} are listed in *Table* 6. From the *Table* 6, we can see that calculated values of the μ_{tot}, α_{tot} and β_{tot} slightly depend on the size of basis sets. Obtained values of the μ_{tot}, α_{tot} and β_{tot} with 6-31G(d) basis set are smaller than those obtained with large size of basis sets. It was found that the calculated results for the basis sets from 6-31+G(d) to 6-311++G(d,p) have minor differences from each other.

It can be seen from the *Table* 6, the calculated values of β_{tot} for the title compound (I) are greater than urea (the β_{tot} of urea is 0.3728×10^{-30} cm^5/esu obtained by 6-31G(d) method). When it is compared with the similar Schiff base compounds in literature, the calculated values of β_{tot} of (I) are smaller than that of 2-methyl-6-[2-(trifluoromethyl)phenyliminomethyl]phenol ($\beta_{tot} = 8.256\times10^{-30}$ cm^5/esu),[44] 4-(2,3-dichlorobenzylideneamino)antipyrine ($\beta_{tot} = 25.191\times10^{-30}$ cm^5/esu)[45] and N-2-Methoxyphenyl-2-oxo-5-nitro-1-benzylidenemethylamine ($\beta_{tot} = 35.072\times10^{-30}$ cm^5/esu)[46] calculated with B3LYP/6-31G(d) method.

The calculated values of β_{tot} and HOMO–LUMO gap for (I) and similar Schiff base compounds[44–46] are given in *Table* 7. From the *Table* 7, as seen from the β_{tot} values for these compounds, there is an inverse relationship between the first hyperpolarizability and HOMO–LUMO gap, allowing the molecular orbitals to overlap to have a proper electronic communication conjugation, which is a marker of the intramolecular charge transfer from the electron donating group through the π-conjugation system to the electron accepting group.[47,48]

Thermodynamic Properties

The standard thermodynamic functions: heat capacity ($C^0_{p,m}$), entropy (S^0_m) and enthalpy (H^0_m) based on the vibrational analysis using the B3LYP/6-31G(d) level to investigate thermodynamical properties of the title compound were calculated and listed in *Table* 8. The standard heat capacities, entropies, and enthalpies increase at any temperatures from 200.00 to 450.00 K for the compound (I),

***Table* 6.** Total dipole moment (μ), polarizability (α), and first hyperpolarizability (β) of the title compound

Basis set	μ (Debye)	α (Å^3)	β (cm^5/esu)×10^{-30}
6-31G(d)	1.776	27.525	3.752
6-31+G(d,p)	1.830	31.407	5.824
6-31++G(d,p)	1.821	31.496	5.879
6-311+G(d)	1.839	31.305	5.751
6-311++G(d,p)	1.809	31.594	5.814

***Table* 8.** Thermodynamic parameters of the title compound: heat capacity ($C^0_{p,m}$), entropy (S^0_m) and enthalpy (H^0_m) based on the vibrational analysis at different temperatures at the B3LYP/6–31G(d) level

T(K)	H^0_m (kcal/mol)	$C^0_{p,m}$ (cal/mol K)	S^0_m (cal/mol K)
200	5.09	40.46	106.96
250	7.44	49.65	117.42
298.15	10.15	58.71	127.29
300	10.26	59.06	127.66
350	13.55	68.31	137.77
400	17.28	77.12	147.74
450	21.45	85.29	157.54

***Table* 7.** The comparison of the values of HOMO–LUMO gap and first hyperpolarizability (β) for similar Schiff base compounds (at B3LYP/6-31G(d) level)

Compound	Gap (eV)	β (cm^5/esu) × 10^{-30}
The title compound (I)	4.082	3.752
2-methyl-6-[2-(trifluoromethyl)phenyliminomethyl]phenol[46]	4.010	8.256
4-(2,3-dichlorobenzylideneamino)antipyrine[47]	3.903	25.191
N-2-Methoxyphenyl-2-oxo-5-nitro-1-benzylidenemethylamine[48]	3.253	35.072

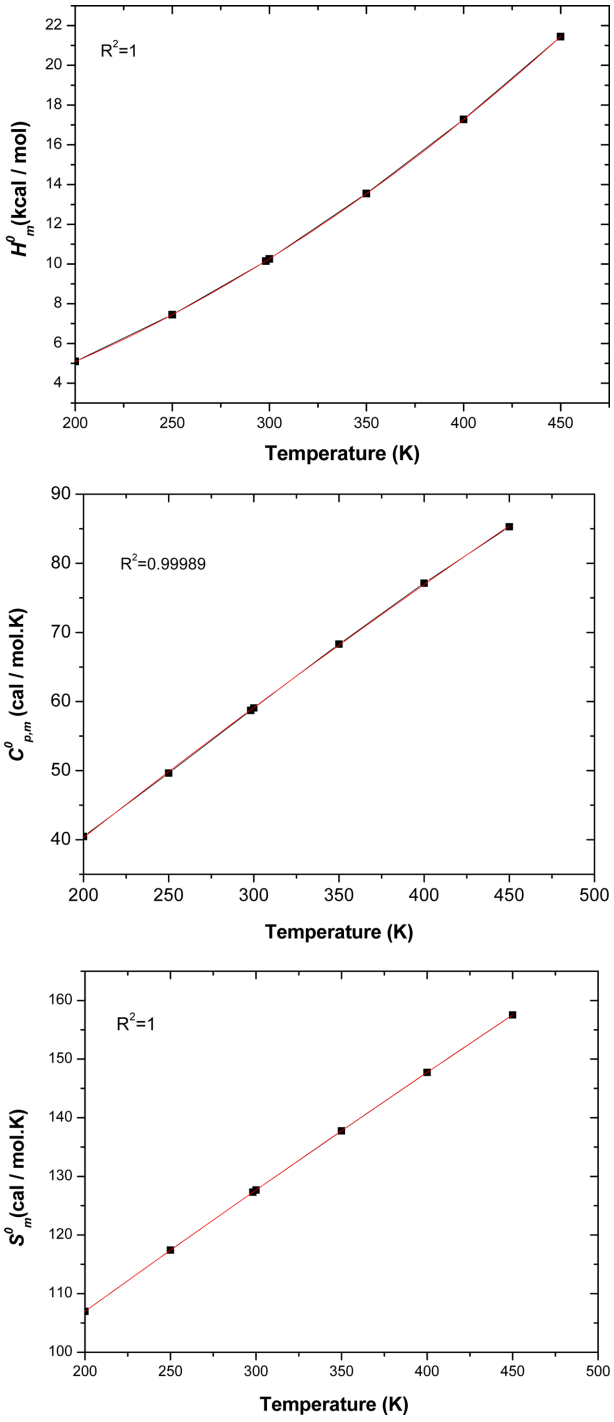

***Figure* 4.** Correlation graphics of thermodynamic properties and temperatures of the title compound.

by reason of the intensities of the molecular vibration increase with increasing temperature. The correlations between the thermodynamic properties $C^0_{p,m}$, entropy S^0_m and enthalpy H^0_m and temperatures T are described and shown in *Fig.* 4, according to the data in *Table* 8.

The correlation equations between these thermodynamic properties and temperature T are as follows:

$$C^0_{p,m} = -0.40732 + 0.21384T - 5T^2 \times 10^{-5} \ (R^2=0.99989) \quad (5)$$

$$S^0_m = 63.70069 + 0.22261T - 3T^2 \times 10^{-5} \ (R^2=1) \quad (6)$$

$$H^0_m = 0.19506 + 0.00623T + 9T^2 \times 10^{-5} \ (R^2=1) \quad (7)$$

The values of $C^0_{p,m}$, S^0_m and H^0_m can easily be obtained at any temperatures using these relationships and these results will be helpful for the further studies of the title compound.

CONCLUSION

Density functional calculations have been successfully performed for the title compound of N-(2,5-methylphenyl)salicylaldimine (I) and the calculated results show that B3LYP/6-31G(d) method can reproduce the title compound very well.

In conclusion, following results can be summarized: (i) The optimized parameters (bond lengths, bond angles, and dihedral angles) of the title compound (I) have been obtained by using the B3LYP/6-31G(d) method. The calculated geometric parameters are, in general, in good agreement with the X-ray structure. (ii) To investigate the tautomeric stability of (I), as seen from calculations, the total energy of the enol form is lower than the keto form, whereas chemical hardness of the enol form is greater than the keto one, which indicates that the enol form of (I) is more stable than its keto form in gas-phase. Also, the total molecular energies obtained by PCM method decrease with the increasing polarity of the solvent and the stability of the title compound increase in going from the gas-phase to the solution-phase. (iii) The MEP map shows that the negative potential sites are on electronegative atoms as well as positive potential sites are around the hydrogen atoms. These sites give intramolecular interactions. For the MEP surface in the studied molecule the weak negative region associated with N1 atom and also the weak positive region by the nearby H1 atom are indicative of an intramolecular (O1–H1···N1) hydrogen bonding. (iv) The NBO analysis is more compatible with the crystal structure of the title compound and it's a very useful method for molecular modelling. In the compound (I), the NBO analysis revealed that the N1(O1)→σ(O1–H1) interaction gives the strongest stabilization to the system by 43.90 kcal mol^{-1}. Electron donating from N1 LP(1) to antibonding (O1–H1) is the most important interaction energy

resulting stabilization of 43.90 kcal mol^{-1}, and this interaction implies the existence of intramolecular hydrogen bond, which was observed experimentally. (v) Computational approach allows the determination of molecular non-linear optical (NLO) properties as an inexpensive way to design molecules by analyzing their potential before synthesis. In addition to the well known empirical rules to estimate qualitatively, the microscopic nonlinear response in organic molecules, especially ab initio B3LYP calculations allow a more accurate prediction of the NLO activity. Our computational results yield that β_{tot} for the title compound (I) is greater than those of urea. It is also compared with the similar Schiff base compounds in literature, the calculated values of β_{tot} of (I). There is an inverse relationship between first hyperpolarizability and HOMO–LUMO gap. (vi) The thermodynamic properties, $C_{p,m}^0$, S_m^0 and H_m^0 and temperatures T were also obtained. The results show that the standard thermodynamic functions increase at any temperatures from 200 to 450 K, because the intensities of the molecular vibration increase with increasing temperature.

Our density functional calculations for the title compound of N-(2,5-methylphenyl)salicylaldimine (I) and the calculated results will be helpful for the design and synthesis of new materials.

Acknowledgments. I thank Dr. Hamit ALYAR (Çankırı Karatekin University, Faculty of Science, Department of Physics, Çankırı-Turkey) for access to the Gaussian 03 program package. And the publication cost of this paper was supported by the Korean Chemical Society.

REFERENCES

1. Emregul, K. C.; Duzgun, E.; Atakol, O. *Corros. Sci.* **2006**, *48*, 3243.
2. Drozdzak, R.; Allaert, B.; Ledoux, N.; Dragutan, I.; Dragutan, V.; Verpoort, R. *Coord. Chem. Rev.* **2005**, *249*, 3055.
3. Yang, C. J.; Jenekhe, S. A. *Macromolecules* **1995**, *28*, 1180.
4. Destri, S.; Khotina, I. A.; Porzio, W. *Macromolecules* **1998**, *3*, 1079.
5. Zeyrek, C. T.; Elmali, A.; Elerman, Y. *Z. Naturforsch.* **2005**, *60b*, 520.
6. Larkin, D. R. *J. Org. Chem*. **1990**, *55*, 1563.
7. Vanco, J.; Svajlenova, O.; Racanska, E.; Muselik, J.; Valentova, J. *J. Trace Elem. Med. Biol*. **2004**, *18*, 155.
8. Taggi, A. E.; Hafez, A. M.; Wack, H.; Young, B.; Ferraris, D.; Lectka, T. *J. Am. Chem. Soc*. **2002**, *124*, 6626.
9. Ramnauth, R.; Al-Juaid, S.; Motevalli, M.; Parkin, B. C.; Sullivan, A. C. *Inorg. Chem.* **2004**, *43*, 4072.
10. Hadjoudis, E.; Vitterakisp, M.; Mavridis, I. M. *Tetrahedron* **1987**, *43*, 1345.
11. Xu, X. X.; You, X. Z.; Sun, Z. F.; Wang, X.; Liu, H. X. *Acta Crystallogr.* **1994**, *C50*, 1169.
12. Dürr, H. *Angew. Chem. Int. Ed. Engl*. **1989**, *28*, 413.
13. Dür, H.; Bouas-Laurent, H. *Photochromism: Molecules and Systems*; Elsevier: Amsterdam, 1990.
14. Schaumburg, K. et al. In *Nanostructure Based on Molecular Materials*; Göpel, W., Ziegler, C., Eds.;Willey-VCH: Weinheim, German, 1992.
15. Özek, A.; Albayrak, Ç.; Odabaşoğlu, M.; Büyükgüngör, O. *Acta Crystallogr*. **2007**, *C63*, 177.
16. Elmali, A.; Kabak, K.; Kavlakoglu, E.; Elerman, Y.; Durlu, T. N. *J. Mol. Struct*. **1999**, *510*, 207.
17. Ünver, H.; Kabak, M.; Zengin, M.; Durlu, T. N. *J. Chem. Crystallogr.* **2001**, *31*, 203.
18. Ünver, H.; Karakaş, A.; Elmali, A. *J. Mol. Struct*. **2004**, *702*, 49.
19. Karakaş, A.; Elmali, A.; Ünver, H.; Svoboda, I. *J. Mol. Struct.* **2004**, *702*,103.
20. Blanchard-Desce, M.; Runser, C.; Fort, A.; Barzoukas, M.; Lehn, J. M.; Bloy, V.; Alain, V. *Chem. Phys*. **1995**, *199*, 253.
21. Karakaş, A.; Elmali, A.; Ünver, H. *J. Nonlinear Optic. Phys. Mat.* **2007**, *16*, 91.
22. Sebastian, S.; Sundaraganesan, N.; Karthikeiyan, B.; Srinivasan,V. *Spectrochim. Acta*, *Part A* **2001**, *78*, 590.
23. Kavitha, E.; Sundaraganesan, N.; Sebastian, S.; Kurt, M. *Spectrochim. Acta*, *Part A* **2010**, *77*, 612.
24. Sun, Y. X.; Hao, Q. L.; Yu, Z.X.; Wei, W. X.; Lu, L. D.; Wang, X. *Mol. Phys.* **2009**, *107*, 223.
25. Seiji, I.; Hiroo, F.; Hidetoshi, K.; Makoto, I.; Nobuaki, K. *Bull. Chem. Soc. Jpn*. **2003**, *76*(4), 733.
26. Elmali, A.; Elerman, Y.; Zeyrek, C. T. *J. Mol. Struct.* **1998**, *443*, 123.
27. Frisch, M. J.; et al. *GAUSSIAN 03,* revision E.01; Gaussian, Inc.: Wallingford, CT, 2004.
28. Dennington, R.; Keith, T.; Millam, J. *GaussView*, version 4.1.2; Semichem, Inc.: Shawnee Mission, KS, 2007.
29. Schlegel, H. B. *J. Comput. Chem.* **1982**, *3*, 214.
30. Peng, C.; Ayala, P. Y.; Schlegel, H. B.; Frisch, M. J. *J. Comput. Chem.* **1996**, *17*, 49.
31. Parr, R. G.; Pearson, R. G. *J. Am. Chem. Soc.* **1983**, *105*, 7512.
32. Foresman, J. B.; Keith, T. A.; Wiberg, K. B.; Snoonian, J.; Frisch, M. J. *J. Phys. Chem*. **1996**, *100*, 6098.
33. Glendening, E. D.; Badenhoop, J. K.; Reed, A. E.; Carpenter, J. E.; Weinhold, F. *NBO*, version 3.1; Theoretical Chemistry Institute: University of Wisconsin, Madison, 1995.
34. Jian, F. F.; Zhao, P. S.; Bai, Z. S.; Zhang, L. *Struct. Chem.* **2005**, *16*, 635.
35. Özbek, N.; Kavak, G.; Özcan, Y.; İde, S.; Karacan, N. *J. Mol. Struct.* **2009**, *919*, 154.
36. Geerlings, P.; De Proft, F.; Langenaeker, W. *Chem. Rev.* **2003**, *103*, 1793.
37. Pearson, R. G. *J. Chem. Ed*. **1987**, *64*, 561.
38. Parr, R. G.; Chattaraj, P. K. *J. Am. Chem. Soc.* **1991**, *113*,

1854.
39. Koopmans, T. *Physica* **1933**, *1*, 104.
40. Politzer, P.; Concha, M. C.; Murray, J. S. *Int. J. Quantum Chem.* **2000**, *80*, 184.
41. Schwenke, D. W.; Truhlar, D. H. *J. Chem. Phys*. **1985**, *82*, 2418.
42. Andraud, C.; Brotin, T.; Garcia, C.; Pelle, F.; Goldner, P.; Bigot, B.; Collet, A. *J. Am. Chem. Soc.* **1994**, *116*, 2094.
43. Thanthiriwatte, K. S.; Nalin de Silva, K. M. *J. Mol. Struct. (Theochem)* **2002**, *617*, 169.
44. Tanak, H. *J. Mol. Struct. (Theochem)* **2010**, *950*, 5.
45. Sun, Y. X.; Hao, Q. L.; Wei, W. X.; Yu, Z. X.; Lu, L. D.; Wang, X.; Wang, Y. S. *J. Mol. Struct.* **2009**, *929*, 10.
46. Yavuz, M.; Tanak, H. *J. Mol. Struct. (Theochem)* **2010**, *961*, 9.
47. Ruiz Delgado, M. C.; Hernandez, V.; Casado, J.; Lopez Navarre, J. T.; Raimundo, J. M.; Blanchard, P.; Roncali, J. *J. Mol. Struct. (Theochem)* **2004**, *709*, 187.
48. Abraham, J. P.; Sajan, D.; Shettigar, V.; Dharmaprakash, S. M.; Nemec, I.; Hubert Joe, I.; Jayakumar, V. S. *J. Mol. Struct.* **2009**, *917*, 27.